

Non-equilibrium chemical potential and stress-induced migration of polymers in tubes

D. Jou^{a,c}, M. Criado-Sancho^{b,*}, J. Casas-Vázquez^a

^aDepartament de Física, Universitat Autònoma de Barcelona, 08193 Bellaterra, Catalonia, Spain

^bDepartamento de Ciencias y Técnicas Fisicoquímicas, Universidad Nacional de Educación a Distancia, Senda del Rey 9, 28040 Madrid, Spain

^cInstitut d'Estudis Catalans, Carme 47, 08001 Barcelona, Catalonia, Spain

Received 26 June 2001; received in revised form 26 September 2001; accepted 2 November 2001

Abstract

A non-equilibrium chemical potential depending on the viscous pressure tensor is used to describe shear-induced diffusion in polymer solutions flowing along cylindrical tubes. Our results generalize previous ones in three main aspects: a Flory–Huggins expression for the equilibrium contribution to the chemical potential is used instead of the ideal-gas like expression, the full expression for the steady-state compliance of the solution is taken into account instead of only the polymer contribution, and the influence of the solute molecular mass is explicitly considered. As a qualitatively new result of considerable practical interest, it stands the prediction that in some circumstances, a dynamical instability may appear, which accelerates and enhances the separation process. © 2002 Elsevier Science Ltd. All rights reserved.

Keywords: Non-equilibrium chemical potential; Polymer migration; Flow in tubes

1. Introduction

Stress-induced polymer migration in flowing solutions is a relevant phenomenon in rheology, chromatography and engineering [1–5]. A coupling between viscous pressure and diffusion flux produces a migration of the polymer solute towards the center of tubes and consequently a depletion of solute near the wall that modifies the apparent viscosity of solution. Furthermore, the sensitivity of this phenomenon to the molecular mass makes it the basis of macromolecular separation methods.

One of the topics of theoretical discussion in this field is the role of thermodynamics, in particular, how the flow contributes to the chemical potential. Indeed, many authors [2,3,7,8] have considered that the entropic and energetic changes produced by the stretching of macromolecules under the action of the flow contribute to a thermodynamic force, which drives the migration. For instance, in one of the pioneering approaches in this line [2], a binary fluid mixture, initially spatially homogeneous in concentration, was subjected to a stress field which produces a thermodynamic driving force for diffusion of macromolecules toward the zones of lower stress (namely, the central region of the tube). This force was taken as the gradient of a potential V as

$\mathbf{F} = -\nabla V$; it produces a stress-induced flux given by

$$\mathbf{J}_s = -\frac{Dc}{RT}\nabla V \quad (1)$$

where D is the diffusion coefficient, c the polymer concentration and R and T have the usual meaning of the ideal-gas constant and absolute temperature, respectively.

On the other hand, concentration inhomogeneities due to this flux produce a diffusion flux described by the classical Fick's law $\mathbf{J}_F = -D\nabla c$. The net flux is then

$$\mathbf{J} = -D\left[\nabla c + \frac{c}{RT}\nabla V\right] \quad (2)$$

In Ref. [2], the expression adopted for the potential V was related to the free energy of extension of Gaussian chains, given by Ref. [10]

$$\Delta F_{\text{flow}} = -\frac{c}{2}RT\left[\ln\left(\det\frac{\mathbf{P}^\nu}{cRT}\right) - \text{Tr}\left(\frac{\mathbf{P}^\nu}{cRT} - \mathbf{U}\right)\right] \quad (3)$$

in such a way that $V = \partial\Delta F_{\text{flow}}/\partial c$. There, \mathbf{P}^ν is the viscous pressure tensor acting on the polymer and \mathbf{U} the unit matrix. This model accounts for how the stretching and the orientation of the macromolecules due to the flow modify the free energy of the solution and was able to describe stress-induced migration leading to an accumulation of polymer near the center of the tube where the stretching of the

* Corresponding author.

macromolecules is minimum because of the vanishing velocity gradient.

The previous model yields for the steady-state concentration profile, obtained from the condition $\mathbf{J} = 0$, the equation

$$\nabla c + \frac{c}{RT} \nabla V = 0. \quad (4)$$

The qualitative trends of this model are satisfactory. However, it is convenient to go beyond it in several aspects. For instance, this model was proposed ad hoc for this physical situation: it would be useful to derive it from a general thermodynamic framework, which could give it a more consistent physical justification and might suggest more applications. From such a more general perspective, it would be easier to evaluate the role of thermodynamic contributions to stress-induced migration, which has led to several controversies (see, for instance, arguments against it in Refs. [11–13] and in support for it in Refs. [5–9]).

In this paper, we revisit the thermodynamic point of view from the perspective of extended irreversible thermodynamics (EIT) [5,14–17]. This theoretical framework is wider than the heuristic treatment in Ref. [2] and its predictions for shear-induced phase separation are found to be qualitatively satisfactory [5,18–21]. Finally, recent applications to shear-induced diffusion in cone-and plate experiments [22,24] have indicated that, due to a thermodynamic instability, shear-induced separation is much accelerated with respect to the predictions of the classical models, in accordance with experimental results. Therefore, it seems appropriate to apply this formalism to tube flows, which have much practical interest.

2. Non-equilibrium chemical potential

In EIT, the thermodynamic quantities are assumed to depend on their local equilibrium variables and also on the fluxes. In the situation being analyzed here, the constitutive equation for the diffusion flux turns out to be [5,17,21]

$$\mathbf{J} = -\tilde{D} \nabla \mu - \frac{D}{RT} \nabla \cdot \mathbf{P}^v \quad (5)$$

with \tilde{D} a coefficient related to D as $D = \tilde{D}(\partial \mu_{\text{eq}}/\partial c)$ with $\mu_{\text{eq}}(T, P, c)$ the local-equilibrium chemical potential and μ a non-equilibrium chemical potential which depends on \mathbf{P}^v as well as on the concentration c , pressure p and temperature T , and which takes the form [20,21]

$$\mu = \mu_{\text{eq}}(T, P, c) + \frac{1}{4} \left(\frac{\partial(VJ)}{\partial n_2} \right)_{T, n_1, \mathbf{P}^v} \mathbf{P}^v : \mathbf{P}^v \quad (6)$$

with n_2 the number of moles of solute and J the steady-state compliance.

Predictions of Eqs. (5) and (6) have been analyzed in detail in the context of shear-induced shift of the critical point in polymer solutions [18–21] and in stress-induced migration in cone-and-plate experiments [22,24] and are

satisfactory. Now, we apply Eqs. (5) and (6) to the flow of dilute polymer solutions in straight cylindrical tubes of circular section. Recall that the only non-vanishing components of the viscous pressure tensor in this situation are [23] $P_{rz} = P_{zr} = -\eta \dot{\gamma}$, $P_{zz} = (N_1 + N_2) \dot{\gamma}^2$, $P_{rr} = N_2 \dot{\gamma}^2$, where η is the shear viscosity, N_1 and N_2 the normal-stress coefficients of the solution and $\dot{\gamma}$ the shear rate. We shall give attention, as in earlier works, to upper-convected Maxwell fluids, for which $N_1 = 2\tau\eta$ and $N_2 = 0$, τ being an average viscoelastic relaxation time of the pressure tensor [10]. In this case, it turns out that the radial component of $\nabla \cdot \mathbf{P}^v$ is zero. Indeed,

$$(\nabla \cdot \mathbf{P}^v)_r = \frac{1}{r} \frac{\partial}{\partial r} (r P_{rr}^v) + \frac{1}{r} \frac{\partial}{\partial \theta} P_{\theta r}^v + \frac{\partial}{\partial z} P_{zr}^v - \frac{P_{\theta\theta}^v}{r} = 0 \quad (7)$$

because $P_{rr} = P_{\theta\theta} = P_{\theta r} = 0$ and P_{zr} does not depend on z . This is an important difference with respect to cone-and-plate flows, where the term $\nabla \cdot \mathbf{P}^v$ is different from zero and points towards the axis of the device, thus promoting a migration of the particles towards the center of the tube according to Eq. (6).

Thus, in the situation studied here, Eq. (5) reduces to $\mathbf{J} = -\tilde{D} \nabla \mu$ and introducing Eq. (6) in Eq. (5), it follows that

$$\mathbf{J} = -\tilde{D} [\nabla \mu_{\text{eq}} + \nabla(\Delta \mu_{\text{flow}})] \quad (8)$$

where $\Delta \mu_{\text{flow}} = \mu - \mu_{\text{eq}}$ is the flow contribution to the chemical potential.

Furthermore, if one assumes, as in Ref. [2], that

$$\mu_{\text{eq}} = \mu_{\text{eq}}^0(T, P) + RT \ln c, \quad (9)$$

then Eq. (8) becomes Eq. (2) with V identified as $\Delta \mu_{\text{flow}}$. In the present analysis, expression (9) for the chemical potential, which is excessively simplistic, will be substituted by the Flory–Huggins expression, which is much more suitable for the description of polymer solutions (see Appendix A).

Another new aspect of the present paper with respect to previous bibliography on this problem will be the inclusion of a more realistic expression of the steady-state compliance appearing in Eq. (6). Instead of taking only the polymer contribution $J_p = \tau_p/\eta_p = (cRT)^{-1}$, we consider the full expression for the Rouse–Zimm model for dilute polymer solutions which is given by Refs. [5,10]

$$J = \frac{CM_2}{cRT} \left[1 - \frac{\eta_s}{\eta(c)} \right]^2 \quad (10)$$

where M_2 is the molecular mass of the polymer, η_s the viscosity of the solvent, $\eta(c)$ the viscosity of the solution and the constant C takes the values 0.4 in the Rouse model and 0.206 in the Zimm model.

Using J instead of J_p has drastic consequences: it predicts a shear-induced shift of the critical point towards upper values of the temperature [5,18–21] (as observed in Ref. [7]) whereas J_p yields a shift towards lower temperatures, in contrast with the experiments. In Appendix A, the experimental parameters appearing in the Flory–Huggins

expression and in J are provided for solution of polystyrene solved in oligomeric polystyrene studied in this paper.

3. Steady-state concentration profile

In the steady-state, $\mathbf{J} = 0$ and therefore, according to Eq. (8), one must have

$$\nabla(\mu_{\text{eq}} + \Delta\mu_{\text{flow}}) = 0 \quad (11)$$

i.e.

$$\mu_{\text{eq}}(c) + \Delta\mu_{\text{flow}}(c, \mathbf{P}^v) = \text{const.} \quad (12)$$

where the constant does not depend on the radial position r . The explicit expression of the non-equilibrium chemical potential, Eq. (6), is derived in Appendix A and allows us to write Eq. (16) in the form

$$\mu_{\text{eq}} + \frac{C\nu_1 M_2 [\eta]}{4RT} \times \left[\frac{M_2 [\eta]}{\nu_1} \frac{\Phi(\bar{c})}{\bar{c}} 2 \left(\frac{M_2 [\eta]}{\bar{c}\nu_1} - m \right) \frac{P_5(\bar{c})}{P_6(\bar{c})} \right] \mathbf{P}^v : \mathbf{P}^v = \text{const.} \quad (13)$$

where all the symbols appearing in the later equation are defined in Appendix A and $\mathbf{P}^v : \mathbf{P}^v$ is given by

$$\mathbf{P}^v : \mathbf{P}^v = 2P_{rz}^2 + P_{zz}^2 = 2\eta^2 \dot{\gamma}^2 + (2\tau\eta)^2 \dot{\gamma}^4. \quad (14)$$

For Newtonian flow ($\tau = 0$) and η independent of concentration, one has a parabolic velocity profile for which $\dot{\gamma}$ depends on the radial position as

$$\dot{\gamma}^2 = \frac{4v_m^2}{R^4} r^2 = \beta r^2 \quad (15)$$

where v_m is the maximum velocity and R the radius of the tube. The parameter β can be also written as $\beta = 16Q^2/\pi^2 R^8$, Q being the total flow rate. Here we assume, as in Ref. [2], that the velocity profile remains parabolic regardless of the concentration redistribution and of non-Newtonian effects. Thus, for consistency, we will assume small values of $\dot{\gamma}$ (i.e. $\tau\dot{\gamma} < 1$), in a first approximation.

In order to determine the constant appearing in Eq. (13), for a given value of parameter Q/R^3 , the concentration profile must satisfy the mass conservation condition

$$\int_0^1 \frac{c(x)}{c_0} x \, dx = \frac{1}{2} \quad (16)$$

being $x = r/R$ and c_0 the initial equilibrium concentration.

In Fig. 1, it is shown that the non-equilibrium chemical potential (13) as a function of the concentration for several values of Q/R^3 for a solution of polystyrene of molecular mass 2000 kg mol⁻¹ solved in an oligomeric polystyrene of molecular mass 0.5 kg mol⁻¹. The point C, where the several curves cross each other corresponds to the concentration for which the values of the coefficient on the term

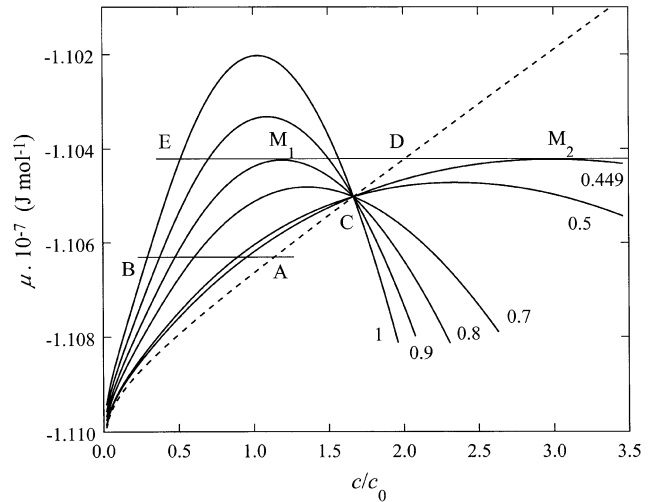


Fig. 1. Chemical potential of polystyrene solved in oligomeric polystyrene as a function of concentration (c_0 is the equilibrium concentration) when the parameter Q/R^3 takes the value 0.1772 s^{-1} . The continuous curves correspond to several values of $x = r/R$. The dashed curve corresponds to the Flory–Huggins model (equilibrium situation).

$\mathbf{P}^v : \mathbf{P}^v$ in Eq. (13) vanishes; thus, at this value of the concentration, the chemical potential does not depend on shear rate. Each horizontal line lower than point C intersects the curves corresponding to the several values of x and gives for each of them a value of the concentration, thus yielding to a possible concentration profile. Point A corresponds to the concentration in the center of the tube, where $\dot{\gamma} = 0$, and point B to $x = 1$, i.e. to the concentration at $r = R$. However, the only acceptable profiles are those satisfying the normalization condition (16), which for each value of Q/R^3 , will fix the position of the point A. Examples of concentration profiles obtained by this method are shown in Fig. 2, for several values of Q/R^3 .

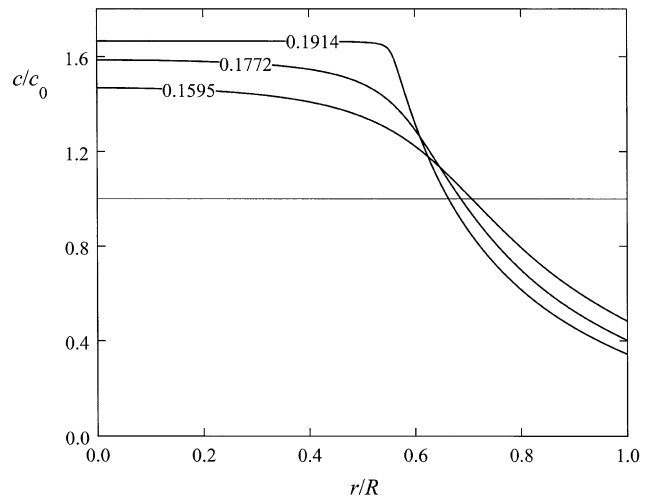


Fig. 2. Concentration profiles of the solute as a function of radial position in the tube for several values of Q/R^3 (in s^{-1}). The horizontal line corresponds to the initial homogeneous profile, which would be stationary if the fluid were at rest ($Q = 0$).

For the horizontal line across C, the concentration profile corresponds to a constant concentration for low values of x , for which the curves of μ satisfy $\partial\mu/\partial c > 0$ at point C. When $\partial\mu/\partial c$ becomes negative at this point, implying that it becomes thermodynamically unstable, the concentration will correspond not to that at C but to the other intersection with the curves of μ , satisfying $\partial\mu/\partial c > 0$. This yields a concentration profile having the form of a central plateau and a decreasing concentration near the border. The behavior just described is shown in the curve with label 0.1914 in Fig. 2. For horizontal lines above C, there appear stability problems, which will be discussed in Section 4.

In Fig. 3, it is shown that the influence of the molecular mass of the solute on the profile for given values of Q/R^3 and the reduced initial concentration \tilde{c}_0 (defined in Appendix A). It is seen that the higher the molecular mass is, the higher is the concentration in the central region. This dependence on the molecular mass could be the basis of chromatographic separation methods.

4. Separation rate

Another important feature is the separation rate. Indeed, if the separation is slow, the length of the tubes required to observe the steady concentration profile must be very long, and the separation process is inefficient. Some of the existing evaluations predict in fact a slow separation. In Ref. [22], we studied the shear-induced separation process in a cone-and-plate device and we found that for high enough shear rates, an instability occurs which accelerates very much the separation with respect to the predictions based on the local-equilibrium chemical potential. In tubes, a similar phenomenon may arise, as commented in this section, which may be of much practical interest.

By combining the mass conservation equation and the expression for the diffusion flux, the evolution of the

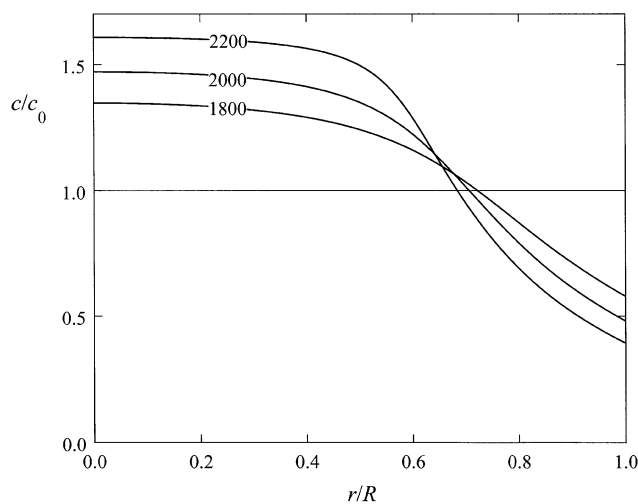


Fig. 3. Concentration profiles for different values of the macromolecular mass of the solute for $Q/R^3 = 0.16 \text{ s}^{-1}$ and $\tilde{c}_0 = 0.26$.

concentration profile is described by

$$\frac{\partial \tilde{c}}{\partial t} = \nabla \left(D_{\text{eff}} \nabla c + \tilde{D} \frac{\partial \Delta \mu}{\partial \dot{\gamma}^2} \nabla \dot{\gamma}^2 \right) \quad (17)$$

Here, we have written the diffusion flux as

$$\mathbf{J} = -\tilde{D} \nabla \mu = -\tilde{D} \left(\frac{\partial \mu_{\text{eq}}}{\partial \tilde{c}} + \frac{\partial \Delta \mu}{\partial \tilde{c}} \right) \nabla \tilde{c} - \tilde{D} \frac{\partial \Delta \mu}{\partial \dot{\gamma}^2} \nabla \dot{\gamma}^2 \quad (18)$$

and define the effective diffusion coefficient D_{eff} as

$$\begin{aligned} D_{\text{eff}} &= \tilde{D} \left(\frac{\partial \mu_{\text{eq}}}{\partial \tilde{c}} + \frac{\partial \Delta \mu}{\partial \tilde{c}} \right) \nabla \tilde{c} \\ &= D \left[1 + \left(\frac{\partial \mu_{\text{eq}}}{\partial \tilde{c}} \right)^{-1} \left(\frac{\partial \Delta \mu}{\partial \tilde{c}} \right) \right] \nabla \tilde{c}. \end{aligned} \quad (19)$$

The term $\nabla \dot{\gamma}^2$ in Eq. (18) yields the flow of particles towards the zone with lower values of the shear rate (provided $\partial\mu/\partial\dot{\gamma}^2$ is positive). This accounts for the tendency of the particles to move towards the center of the tube. In usual conditions, when $D_{\text{eff}} > 0$, this flux towards the center is opposed by the tendency to homogenization due to diffusion. However, in some situations (for values of \tilde{c} and \mathbf{P}^v in certain regions) D_{eff} may become negative. In this case, the term enhances the separation, rather than opposing to it, and the separation becomes much faster. This may be a very interesting feature from the practical point of view, because it both accelerates separation and enhances the concentration near the axis.

Of course, D_{eff} negative corresponds to an unstable situation. Therefore, it will only last a short period, until the separation has arrived to concentrations where D_{eff} becomes again positive everywhere. In Fig. 4, the dashed curve corresponds to D_{eff} equal to zero and the concentration profile is

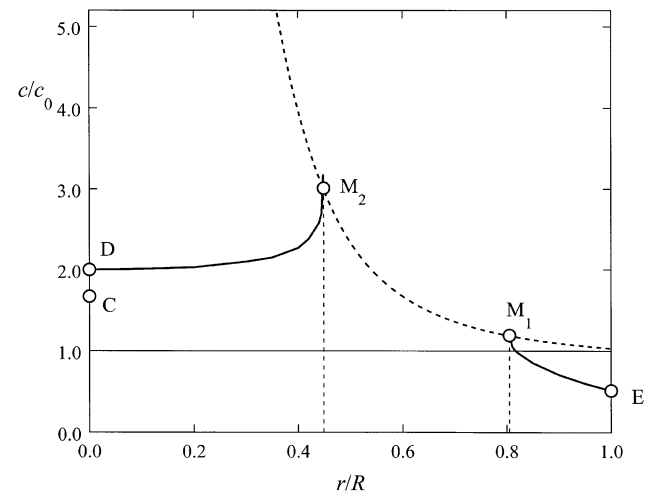


Fig. 4. The dashed curve indicates the line where the effective diffusion coefficient (19) becomes zero and the solution becomes unstable. The continuous curves between D and M_2 and between M_1 and E correspond to the concentration profile, which vanishes in the region between M_2 and M_1 . Then, there would be a high accumulation of the solute in the central region and a much lower accumulation in the layer near the wall. The physical reality of the later is, for the moment, speculative.

shown as a continuous line. This concentration profile corresponds to a horizontal line above the point C in Fig. 1. For low values of x (i.e. in the central region), the concentration increases with the radius. This is due to the fact that in this zone $\partial\mu/\partial\dot{\gamma} < 0$ in such a way that the inhomogeneity in $\dot{\gamma}$ drives a flux towards zones with higher shear rate, in contrast with the situations depicted in Fig. 2. This behavior is stable in the region with $D_{\text{eff}} > 0$, whereas when $D_{\text{eff}} = 0$, (i.e. $\partial\mu/\partial c = 0$) the profile becomes unstable. According to Fig. 4, this instability appears between the points M_1 and M_2 , which correspond to $\partial\mu/\partial c = 0$ in Fig. 1. From M_1 to the border of the cylinder, the situation becomes again stable, as D_{eff} becomes again positive and the profile is decreasing, because in this region $\partial\mu/\partial\dot{\gamma}^2 > 0$, whereas the concentration vanishes between M_1 and M_2 . From a physical point of view, this behavior implies a strong concentration of the solute in the central region and maybe a tenuous presence of solute near the walls.

The concavity of the concentration profile near the axis could be obscured in the practice by the non-vanishing value of the gyration radius of the macromolecules, which would tend to homogenize this central region. The outer part of the profile could be of interest in medical situations affecting the walls of veins or arteries, but for the moment, this is still speculative, in contrast with the concentration in the central zone, which is qualitatively observed.

5. Conclusions

We have generalized earlier models of shear-induced diffusion in tubes, by using the shear-dependent chemical potential as derived from the framework of EIT. The main differences from the earlier model by Tirrell and Malone [2] are the following ones:

1. In Ref. [2], the chemical potential leading to migration is introduced ad hoc, though a microscopic model justifies it. In our paper, the same effects are directly included in a non-equilibrium chemical potential, which has been used in a rather general context and in several other applications [5,18–22].
2. We have taken into account detailed experimental information for the physical parameters and functions appearing in the analysis for a solution of polystyrene in oligomeric polystyrene, in particular, we have considered explicitly the influence of the molecular mass of solute, which is important in separation methods.
3. As in Ref. [2], our analysis shows that the shear flow induces a migration of the solute towards the center of the tube and corroborates the results by the above-mentioned authors, but with more realistic details about the equilibrium form of the chemical potential and of the steady-state compliance. The concentration profiles shown in Fig. 2 have a similar form to the profiles in fig. 3 of Ref. [2]. Indeed, Tirrell and Malone parametrize their curves in terms of the dimensionless quantity $\alpha =$

$(32/3\pi)(Q/R^3)\dot{\gamma}^2$; the curves in Fig. 2 of the present paper correspond to values of α between 5 and 10, when one uses for τ relaxation times of the order of that reported in Ref. [24] for the system we have studied.

4. An especially interesting prediction of our model, not present in the simpler formulation in Ref. [2] is that, beyond a critical value of the shear rate and of concentration the system becomes thermodynamically unstable, with a negative value of an effective diffusion coefficient. This has two main effects: it accelerates the separation process and it enhances the accumulation of solute in the central region (between points D and M_2). This could be very interesting from a practical perspective, because it would indicate the possibility of a more efficient separation, in a shorter time and with shorter tubes. However, a detailed study of this regime would require to go beyond the assumption of a parabolic velocity profile.

These instability effects, discussed in Section 3, are analogous to those experimentally found in cone-and-plate devices [22,25], where the observed separation rate is two orders of magnitude faster than that predicted by local-equilibrium thermodynamics, but compatible with the predictions of our formalism [22]. Thus, the present analysis together with that in Ref. [21], describes in a unified way the shear-induced migration both in tubes and in cone-and-plate flows, with the common feature of a faster separation, which implies that this process may have more practical interest than those from previous analyses.

Though our approach is essentially macroscopic, it may be interesting to provide a microscopic image of the reasons for the migration. First of all, it is convenient to recall that the viscous pressure tensor is directly related to the macromolecular configuration tensor [10], which is usually taken as an internal variable in alternative thermodynamic descriptions of flowing polymer solutions [13,26–29]. Thus, under the action of the viscous pressure, the macromolecules will become stretched (higher internal energy) and more oriented (less entropy) than in absence of the viscous pressure, in such a way that their free energy is higher in the zones with higher shear rate. Thus, the macromolecules will tend to migrate towards regions with lower shear rate, i.e. near the center of the tube. This is the usual microscopic explanation, which corresponds to the last term in Eq. (18). Besides this contribution, we also include in our analysis the concentration dependence of the non-equilibrium part of the chemical potential, i.e. the second term inside the parentheses in the coefficient of the concentration gradient in Eq. (18). This term vanishes in Ref. [2] and in many other analyses based on the simple hypothesis that $J = 1/cRT$, because in the chemical potential (6), the term in c^{-2} coming from $\partial J/\partial c$ is cancelled by the c^2 term coming from $(\mathbf{P}^v)^2 = \eta^2 \dot{\gamma}^2 = (cRT\tau)^2 \dot{\gamma}^2$, yielding a non-equilibrium contribution to the chemical potential (6), which depends on the shear rate but not on the concentration. It is precisely this dependence, which arises in our

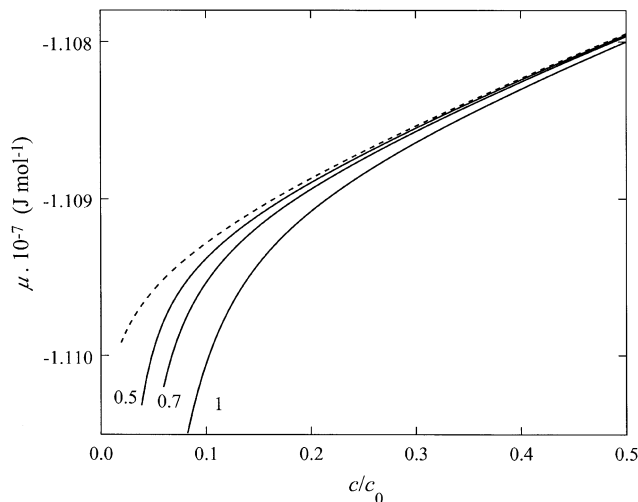


Fig. 5. The same as in Fig. 1 but using $J = (cRT)^{-1}$ for the steady-state compliance instead of the full expression (10). The marked contrast with Fig. 1 and the lack of satisfactory experimental predictions show explicitly the importance of using the full expression (10).

more detailed description of the steady-state compliance (10) and is reflected in the non-monotonic character of the chemical potential as a function of the concentration (Fig. 1), the responsible of the instability examined in Section 4, which does not appear, of course, in the simplified models ignoring such dependence (Fig. 5). In the usual analyses, the tendency of the particles to migrate towards the regions with lower shear rate is compensated by the increase of the chemical potential with concentration in this region; if for a range of values of concentration and viscous pressure the chemical potential *decreases* with increasing concentration, one would have of course an instability. Characterizing this instability from detailed microscopic models is a demanding task for the future, beyond the scope of the present paper.

Acknowledgements

This work has been partially supported by the Dirección General de Investigación Científica y Técnica of the Spanish Ministry of Science and Technology under grant BFM2000-0351-C03-01. Fruitful discussions are acknowledged with Professor L.F. del Castillo from UNAM, México.

Appendix A

In order to derive the explicit expression of the non-equilibrium contribution to the chemical potential introduced in Eq. (6), namely

$$\Delta\mu_{\text{flow}} = \frac{1}{4} \left(\frac{\partial(VJ)}{\partial n_2} \right)_{T, n_1, \mathbf{P}^\nu} \mathbf{P}^\nu : \mathbf{P}^\nu \quad (\text{A1})$$

the functional dependence of V and J on the composition of the system is necessary. According to the cell model, the volume of the solution is given by $V = \nu_1 \Omega$, where ν_1 is the

molar volume of the solvent and the parameter Ω is defined as $\Omega = n_1 + mn_2$ with n_1 and n_2 the number of moles of solvent and of polymer and m the ratio between the molar volumes of the polymer and the solvent. The concentration and volume fraction can be expressed by the respective equations $c = n_2 M_2 / \nu_1 \Omega$ and $\phi = mn_2 / \Omega$.

Using $J = (cRT)^{-1}$ together with (A1)–(A3), we write

$$\Delta\mu_{\text{flow}} = \frac{\nu_1 m [\eta]}{4RT} \tilde{c}^{-1} \left(2 - \frac{M_2 [\eta]}{\nu_1 m} \tilde{c}^{-1} \right) \mathbf{P}^\nu : \mathbf{P}^\nu \quad (\text{A2})$$

where the reduced concentration $\tilde{c} = [\eta]c$, with $[\eta]$ the intrinsic viscosity, has been introduced.

If instead of $J = (cRT)^{-1}$, the Eq. (10) is used in (A1), a functional dependence between viscosity and concentration is required. When the expression proposed in our previous papers [21,22,24] is used

$$\frac{\eta}{\eta_s} = 1 + \tilde{c} + k\tilde{c}^2 \quad (\text{A3})$$

yields the result

$$\begin{aligned} \Delta\mu_{\text{flow}} &+ \frac{C\nu_1 M_2 [\eta]}{4RT} \left[\frac{M_2 [\eta]}{\nu_1} \frac{\Phi(\tilde{c})}{\tilde{c}} + 2 \left(\frac{M_2 [\eta]}{\tilde{c}\nu_1} - m \right) \frac{P_5(\tilde{c})}{P_6(\tilde{c})} \right] \mathbf{P}^\nu \\ &: \mathbf{P}^\nu = \text{const.} \end{aligned} \quad (\text{A4})$$

where the functions $P_i(\tilde{c})$ are

$$\Phi(\tilde{c}) = \tilde{c} \left(\frac{1 + k\tilde{c}}{1 + \tilde{c} + k\tilde{c}^2} \right)^2 \quad (\text{A5})$$

$$P_5(\tilde{c}) = (k-1)\tilde{c}^2 + (k^2 - 3k)\tilde{c}^3 - 3k^2\tilde{c}^4 - k^3\tilde{c}^5 \quad (\text{A6})$$

$$P_6(\tilde{c}) = (1 + \tilde{c} + k\tilde{c}^2)^3. \quad (\text{A7})$$

The equilibrium contribution to the chemical potential (6) is given by the usual Flory–Huggins expression

$$\frac{\mu_{\text{eq}}}{RT} = \ln(1 - \phi) + \left(1 - \frac{1}{m} \right) \phi + \chi\phi^2. \quad (\text{A8})$$

In order to study the solutions considered in Ref. [25] (high molecular mass polystyrene solved in an oligomeric polystyrene whose molecular mass is 0.5 kg mol^{-1}), we use the same numerical values as in Ref. [24]. In particular, the dependence of the intrinsic viscosity and the Huggins constant on the molecular mass is given by Ref. [24] $[\eta] = 2.25 \times 10^{-3} M_2^{0.524}$ and $k = 497.9 M_2^{-0.49}$. These parametrizations are used to derive the molecular mass dependence of the concentration profiles in Fig. 4.

References

- [1] Agarwal US, Dutta A, Mashelkart RA. Chem Engng Sci 1994;49:1693.
- [2] Tirrell M, Malone MF. J Polym Sci: Polym Phys D 1977;15:1569.

- [3] Dutta A, Ravetkar D, Mashelkar RA. *Chem Engng Commun* 1987;53:131.
- [4] Onuki A. *J Phys: Condens Matter* 1997;9:6119.
- [5] Jou D, Casas-Vázquez J, Criado-Sancho M. *Thermodynamics of fluids under flow*. Berlin: Springer, 2000.
- [6] Nozières P, Quemada D. *Europhys Lett* 1986;2:129.
- [7] Metzner AB, Cohen Y, Rangel-Nafaile C. *J Non-Newtonian Fluid Mech* 1979;5:449.
- [8] Cohen Y, Metzner AB. *Rheol Acta* 1986;25:28.
- [9] Casas-Vázquez J, Criado-Sancho M, Jou D. *Europhys Lett* 1993;23:469.
- [10] Bird RB, Curtiss CF, Armstrong RC, Hassager O. *Dynamics of polymeric liquids*, vol. 2. New York: Wiley, 1987.
- [11] Aubert JH, Tirrell M. *J Chem Phys* 1980;72:2694.
- [12] Aubert JH, Prager S, Tirrell M. *J Chem Phys* 1980;73:4103.
- [13] Drouot R, Maugin GA. *Rheol Acta* 1983;22:336.
- [14] Jou D, Casas-Vázquez J, Lebon G. *Extended irreversible thermodynamics 2*. Berlin: Springer, 1996.
- [15] Jou D, Casas-Vázquez J, Lebon G. *Rep Prog Phys* 1999;62:1135.
- [16] Nettleton RE, Sobolev SL. *J Non-Equilib Thermodyn* 1995;20:297.
- [17] Jou D, Casas-Vázquez J, Lebon G. *J Non-Equilib Thermodyn* 1998;23:277.
- [18] Jou D, Casas-Vázquez J, Criado-Sancho M. *Adv Polym Sci* 1995;120:205.
- [19] Criado-Sancho M, Jou D, Casas-Vázquez J. *Macromolecules* 1991;24:2834.
- [20] Criado-Sancho M, Casas-Vázquez J, Jou D. *Phys Rev E* 1997;56:1887.
- [21] Criado-Sancho M, Casas-Vázquez J, Jou D. *Polymer* 1995;36:4107.
- [22] Del Castillo LF, Criado-Sancho M, Jou D. *Polymer* 2000;41:2633.
- [23] Tanner RL. *Engineering rheology*. Oxford: Oxford Science Publications, 1988. p. 85.
- [24] Criado-Sancho M, Jou D, Del Castillo LF, Casas-Vázquez J. *Polymer* 2000;41:8425.
- [25] MacDonald MJ. *J Rheol* 1996;40:259.
- [26] Grmela M, Ottinger HC. *Phys Rev E* 1997;56:6620.
- [27] Lhuillier DL. *J Phys II (France)* 1995;5:19.
- [28] Maugin GA. *The thermomechanics of nonlinear irreversible behaviors*. Singapore: World Scientific, 2000.
- [29] Beris AN, Edwards SJ. *Thermodynamics of flowing fluids with internal microstructure*. Oxford: Oxford University Press, 1994.